SSRG International Journal of Civil Engineering
ISSN: 2348-8352/ https://doi.org/10.14445/23488352/IJCE-V13I4P124

Volume 13 Issue 4, 396-412, April 2026

Original Article

Design of an Integrated IoT-FuzzyAHP Framework for Real-Time Geotechnical Risk Management Using Entropy and Reinforcement Learning-Driven Decision Optimizations

Radhika S. Thakre[1], Uday P. Waghe[2], Yogesh P. Kherde[3], Rajesh M. Bhagat[4], Abhay G. Hirekhan[5], Pallavi B. Gadge[6], Amar Jain[7]

[1,2,3,4]*Department of Civil Engineering, Yeshwantrao Chavan College of Engineering, Nagpur, Maharashtra, India.*
[5]*Department of Civil Engineering, St. Vincent Pallotti College of Engineering & Technology, Nagpur, Maharashtra, India.*
[6]*Department of Civil Engineering, G H Raisoni College of Engineering, Nagpur, India*
[7]*Department of Civil Engineering, Symbiosis Institute of Technology, Symbiosis International (Deemed University), Pune, Maharashtra, India.*

[7]*Corresponding Author : amar.jain@sitpune.edu.in*

Received: 17 January 2026 Revised: 20 February 2026 Accepted: 25 March 2026 Published: 28 April 2026

Abstract *- For effective geotechnical risk management, risk detection must be timely, and priority capacity must prioritize unsafe environmental and terrain dynamics. In the realm of complex terrain processes, existing DSS recognize one specific slope failure using the input model or measured sensor data. Errors and limitations of capability severely affect accuracy. Designing the prospective DSS will be unresolved. This paper has sought to outline the Multi-Layer Decision Support Model (MCDSS) with the support of Fuzzy Analytical Hierarchy in compliance with the Internet of Things and real-time data streaming. The design is such that it allows me to have successive blocks to facilitate easy and somewhat block-wise data flow; that is, it gives the concept of an accurate feedback loop with iterative optimization. The first block looks inside Real-Time IoT Data Collection, where live feed from the wells for soil moisture, pore pressure, safety, and settlement is referred to. This does direct into the Dynamic Entropy-Driven Fuzzy-AHP (DE-FuzzyAHP) module so that the set of the fuzzy membrane function could be adaptively tuned with Shannon entropy, increasing sensitivity over data variability in the said process. The tuned set of weights is improved using the Outcome-Optimized Reinforcement Learning AHP Tuner (OORL-AHP), which will learn weights very quickly by applying Q-learning using field mitigation feedback. Awareness of the learning from the optimization of the retrieval weight and the outcome. These outcomes are embedded in the very Fuzzy-AHP Integrated Bayesian Belief Risk Network (FBBRN) from where the very updated causal risk dependencies and probabilistic forecasts are framed at real timestamp scenarios. During the heightened risk, a triggered alert from the Risk Mapping block-Spatially Adaptive Multi-Resolution Risk Mapping (SAMR-RM) for drone or sensor-assisted high-resolution hotspots will be mapped. Moreover, later, with Ns/Ni, the Decision Confidence Quantification Meta-Layer (DCQML) trains and builds the sensors' reliability, data perturbations, and expert communication into a confidence score in the very process. This is a unified technique for improving the accuracy of risk prioritization (from ~78% to ~95%), setting tension on forecast lead delays, enhancing mapping that adapts, and putting forth quantified decision confidence sets. This represents a new wave of integration that makes entropy movements and machine learning work together seamlessly, with a significant impact on probabilistic risk forecasting and spatial intelligence for new geotechnical risk management.*

Keywords *- Geotechnical Risk, Fuzzy-AHP, IoT Sensors, Bayesian Belief Network, Reinforcement Learning*.

1. Introduction

The occurrence of geotechnical hazards like landslides, ground subsidence, and soil liquefaction represents a constant system of risk to the infrastructural stability and human security, which occurs in areas with intricate topography and changing environmental driving forces. The management of such hazards depends on the ability to effectively respond to these hazards, which is possible through early-detection functions coupled with proper prioritization of the risks and responsiveness in the decisions related to mitigating or accepting the possible outcomes. Nevertheless, geotechnical processes are by their nature time-dependent, as well as intensely space-dependent and interrelated in triggering, which makes applying sound and transferable decision-support policies a daunting

objective. Traditional methods of assessment of geotechnical risk are mainly founded on the frameworks of a static nature, and the findings of both expert knowledge and experience are put together to produce fixed risk scores.

Most of the existing decision support systems, even when sensor data are included, have a largely disconnected or batch-driven approach to processing sensor data, and do not have the mechanisms of continuous learning or adaptive learning through feedback.

Consequently, these models do not dynamically re-assign risk priorities in conditions where monitored parameters extend past critical levels, hence limiting their usefulness in providing real-time warning and on-site decision-making. This disconnect is especially important in situations when all the development is a swift reaction, or prioritization can greatly increase the losses.

The growing access to IoT-based geosensors has opened the range of possibilities to monitor crucial parameters continuously, such as ground moisture, pore water pressure, ground settlement, and seismic activity. Despite this improvement, existing geotechnical decision support systems have exploited little of real-time data streams to provide adaptive risk assessment. The majority of currently used models are either observed sensor and expert-based multi-criteria formulations or use standardized schemes of weightings that do not evolve with changing uncertainty, spatial heterogeneity, or mitigation consequences. As a result, the propagation of uncertainty, temporal variability, and feedback is not well-addressed.

The Multi- Criteria Decision-Making (MCDM) techniques, especially Fuzzy Analytical Hierarchy Process (Fuzzy-AHP), have been actively utilized to address the subjective uncertainty/expert knowledge in the geotechnical applications. Although it is useful when dealing with linguistic ambiguity, conventional Fuzzy-AHP models are, in principle, too rigid and do not respond dynamically to changes in data. Recent machine learning research has increased the predictive power of isolated geotechnical issues, but most do not incorporate learning methods into decision ranking tools or apply probabilistic causal reasoning.

Such gaps suggest the lack of a single, adaptive decision-support architecture, which is able to continually combine sensor measurements, expert knowledge, quantification of uncertainty, and educational experience of previous modification achievements.

To respond to this demand, the current paper suggests a modular, feedback-provided structure, unifying dynamic entropy-based fuzzy modeling, adaptive weight optimization via reinforcement learning, assuming causal propagation of risk and prospects of risk through Bayesian inference, and spatially adaptive risk mapping. The suggested system is intended to transform as data enters it and allows responsible, context-aware, and reliable geotechnical risk decision-making in real-time settings.

1.1. Novelty, Motivation & Contribution

The major inspiration behind the research is the inability of current geotechnical risk assessment frameworks to incorporate changes in field conditions that continuously vary due to the constraints of decision-making frameworks largely based on inactive or semi-robust decision frameworks. Although Fuzzy-AHP, machine learning, or probabilistic models have been used successfully in the past as independent methods, there has not been a comprehensive framework that combines real-time sensing, uncertainty adaptation, learning-based optimization, and causal risk reasoning.

This gap is bridged by the novelty of this work: a fully integrated and multi-layered decision-support architecture. In contrast to the traditional Fuzzy-AHP-based systems, where the membership functions are fixed and together with the criteria weight are constant, the proposed structure supports adaptive dynamical entropy-driven adjustment of fuzzy membership functions, which allows the model to react directly to uncertainty variations in real-time sensor data. It is additionally improved with reinforcement learning weight tuning, where Q-learning and Deep Q-Networks optimize AHP criteria importance through each learning cycle, depending on observed mitigation effects, and thus the feedback loop between decision, action, and performance is closed. Unlike the current machine learning models, which are highly concerned with predicted accuracy, the suggested Method incorporates learning within an organized decision-making process. Static risk modeling. Interdependent geotechnical hazards can be probabilistically modeled using a Fuzzy-AHP-based Bayesian Belief Risk Network (FBBRN), and continuously updated risks are provided by the introduction of new evidence.

Moreover, the Spatially Adaptive Multi-Resolution Risk Mapping (SAMR-RM) module is used to enhance situational awareness, facilitating the targeted high-resolution mapping of the emerging hotspots with the help of mobile sensors and drones. Another input is the proposal of a Decision Confidence Quantification Meta-Layer (DCQML) that directly measures the reliability of the decisions produced by considering sensor stability, data variability, and expert consistency, the latter being a feature that is practically non-existent in the present frameworks. Together, the contributions form a scalable and adaptive geotechnical risk management paradigm, with demonstrable geotechnical risk prioritization errors (improvement to 95%, on average), reaction and forecast time (less than 24 hours), and forecast prediction error (a lead time of 8-10 hours) being comparably better than conventional, fixed, and semi-dynamic models.

2. In-Depth Review of Models Used for Geotechnical Risk Management Analysis

The themes vary based on the daily increase, where debates and segments are filling entry value, a unique and rapidly evolving space of implementation in geotechnical engineering through Machine Learning (ML) and Artificial

Intelligence (AI). Coming out of the deterministic and empirical models, the research field is moving through a paradigm shift that is characterized by data-driven approaches in their ability to manage the complexity, nonlinear, and multivariate nature of earth systems as problems. The earliest of these corpus were the one by Cisneros Eufracio et al. [1]. Their article shows how Quantum Machine Learning (QML) can be used to predict the behavior of rock blocks across structural discontinuities on the basis of potential falling under gravity. This concept would inform the future integration of the new paradigms of computation into the traditional Method of geotechnical analysis. Next in line is the article by Tuwa et al. [2], which utilizes a frequency ratio approach complemented with relevant geotechnical and hazard indicators to predict landslide vulnerability in volcanic regions. That initial section of the timeline has confidence swirling in respect to combining geostatistics with domain-specific pointers and using them to influence the decision-making process. The emphasis advanced on the timeline was, therefore, toward ensemble learning and optimization techniques. Onyelowe et al. [3] give a numerical model that marries debris flow susceptibility analysis and slope stability prediction through metaheuristic training algorithms for performance improvement in the process. Raj et al. [4] extend ML deployment to the prediction of rock fragmentation resulting from blasting using supervised models for performance tuning. A slightly more specialized route is taken by Sharma et al. [5] in predicting soil water characteristic curves, reinforcing the perception that ML methods can adequately handle highly nonlinear soil behavior during their best interpretations of performance. Pan et al. [6] outline the scope of AI as a general application in geotechnics, identifying opportunities as well as systemic challenges in model validation, feature selection, and regulatory alignment sets.

In addition to initial demonstrations, new literature shows a progressive transition of machine learning to geotechnical engineering, from increasingly extensive tasks of isolated prediction to frameworks of applications. The earliest research was mostly concerned with proof-of-concept implementations, but the recent research is on ensemble learning, hybrid physics-data models, and predictions with uncertainty. The reviews and meta-analyses prove that the performance of the models is steadily dependent on the quality of data, feature engineering, and domain constraints instead of algorithm selection. This paradigm shift verifies an objective of coming of age in the field and making of ML not a self-contained prediction mechanism but an inseparable decision-supporting aspect of geotechnical methodology [9, 10, 11, 12, 16, 38].

Table 1. Model's empirical review analysis

Reference	Method	Main Objectives	Findings	Limitations
[1]	Quantum Machine Learning (QML)	Predict rock block fall using structural control and QML	Demonstrated potential of QML in slope failure prediction	High computational complexity
[2]	Frequency Ratio + Geotechnical Analysis	Landslide susceptibility in volcanic terrain	Integrated Method improves hazard delineation	Region-specific calibration needed
[3]	Metaheuristic ML Models	Debris flow susceptibility and slope stability	Effective across multiple terrains	Complex tuning of metaheuristic models
[4]	Supervised ML	Predict rock fragmentation from blasting	High accuracy in real blasting scenarios	Limited by dataset size
[5]	Regression ML Models	Soil water characteristic curve prediction	ML models outperform empirical methods	Performance is dependent on input quality
[6]	Review/Survey	Overview of AI in geotechnical engineering	Identified key challenges and future directions	Does not present a new methodology
[7]	Soft Computing	UCS prediction in soft soils	Improved estimation of UCS values	Less tested across soil types
[8]	ML-Based Classification	Petrographic classification in coalfields	Successful mapping of lithological classes	Narrow geographic application
[9]	Review	Survey of ML in geotechnics	Categorized ML use cases and performance	Lacks model implementation
[10]	Comprehensive Review	ML in geotechnical disaster early warning	ML improves forecast reliability	Limited real-time deployment evidence
[11]	Advanced ML	Landslide susceptibility mapping in Cyprus	High spatial accuracy using geotechnical features	Need for localized training
[12]	Meta-Analysis	Compare ANN, ML, DL, and ensemble methods	Ensemble methods consistently perform best	Computational resource-intensive

[13]	ML for Stabilized Slopes	Nano-silica slope stabilization assessment	Effective risk prediction with ML	Specific to the stabilization method
[14]	GIS + ML	Link geotechnical indexes to landslides	High correlation and predictive power	GIS resolution impacts performance
[15]	GIS-AHP + ML	Map aggregate resource potential	High utility in resource management	Multi-criteria weight sensitivity
[16]	Monotonic ML	Slope stability with constraint-based learning	Improved interpretability and physical consistency	Limited flexibility
[17]	Review	ML techniques in rock slope stability	Identified strengths of various models	No practical validation
[18]	Kernel-Based ML	Liquefaction probability prediction	Effective in seismic zones	Data sparsity in some locations
[19]	Risk Scoring + ML	Pipeline qualitative risk assessment	ML enhances risk quantification	Subjective scoring is still required
[20]	Physics-Informed ML	Resilience modeling for infrastructure	Combines physical laws with ML	High model development cost
[21]	Reliability ML	Risk analysis in geoengineering	Quantitative reliability metrics introduced	Limited field-scale testing
[22]	GUI-based ML	Slope stability prediction under seismic loads	User-friendly interface with high accuracy	Model generalizability untested
[23]	ML Classification	Soil liquefaction behavior	Deep features extracted from geotechnical properties	High dimensionality challenges
[24]	Hybrid FEA + ML	Success prediction of deep excavations	Combines numerical simulation with AI	Training data requirements are high
[25]	Ensemble ML	Enhanced slope stability modeling	Best performance among tested models	Computational overhead
[26]	ML Combination Models	Predict geophysical slope behavior	Boosted robustness using hybrid learning	Complex architecture
[27]	Integrated ML Risk Models	Co-seismic landslide and exposure analysis	Multi-risk integration increases realism	Large dataset requirement
[28]	GIS + ML	Seismic vulnerability mapping in urban areas	Detailed spatial zoning of risks	Dependent on GIS data quality
[29]	DCP + ML	Liquefaction susceptibility via cone penetration	Rapid and reliable predictions	Not yet field-integrated
[30]	SPT/CPT + ML	Liquefaction risk prediction	Good performance across test sites	Manual preprocessing needed
[31]	Physics + ML Integration	Landslide prediction in data-scarce zones	Improves model robustness	Limited in-situ validation
[32]	Model Comparison	Validate ML landslide models	Random forest and XGBoost are the most accurate	No dynamic update mechanism
[33]	Regression ML	Rock strength prediction	Accurate and fast prediction model	Needs more extensive calibration
[34]	DL + Ensemble	Soil liquefaction and classification	Best performance on the benchmark dataset	Black-box interpretation issue
[35]	Random Forest	Landslide susceptibility mapping	Effective for the Himalaya region	Region-specific model
[36]	Benchmarking ML	Slope stability under dynamic load	Outperformed limit equilibrium methods	Limited geotechnical factors
[37]	Review	Drones in geotechnical engineering	Highlight synergy with ML	Limited to data acquisition
[38]	AI Review	AI-enhanced computational mechanics	Proposed future integration pathways	Conceptual review
[39]	ML in Project Management	Claim analysis in construction	ML links claims to performance outcomes	Not specific to geotechnical data
[40]	ML Regression Models	UCS and leachability prediction	Useful for dredged sediment analysis	Specific to the land reclamation context

Iteratively, Next, as per Table 1, At almost the same time, Thapa and Ghani [7] undertake a specific study on unconfined compressive strength prediction using soft computing with a significant emphasis on real-time soil characterizations. An assembly of this kind demonstrates the development of single-purpose models to combined methods in which predictive accuracy is assisted by physical realism of the process. Banerjee et al. [8] take the opportunity to use petrographic classification to demonstrate that machine learning could help stratigraphic delineations in coalfields. In contrast, Harle and Wankhade [9] eloquently summarize the status quo of existing machine learning in geotechnics, making the recent surge in regression, classification, and clustering schemes illuminate. Lin et al. [10] present a systematic review of early warning systems that identify essential ML architectures for forecasting geotechnical disasters. Moving a step further, Tzampoglou et al. [11] incorporate geotechnical parameters into landslide susceptibility mapping using ensemble ML in Cyprus, indicating that local calibration of the model would be essential.

In contrast, Yaghoubi et al. [12] have looked at neural, deep, and ensemble learning approaches and provided a strong meta-analytical background for model selection on earthquake risk. Thapa et al. [13] demonstrated slope stabilization using nanosilica and machine learning. At the same time, a parallel work by Tzampoglou et al. [14] discussed the significance of geotechnical indices correlated with landslide activities using ML-integrated GIS models. Hussain et al. [15] emphasize an amalgamation of the AHP, petrographic, and ML methods for the mapping of aggregate resource potential, providing evidence for the centric importance of multi-criteria analysis in predictive geotechnical frameworks. As a more formal approach to the integration of expert knowledge into learning algorithms, with the introduction of monotonic constraints by Pei and Qiu [16], a formal mechanism is created to encode expert knowledge into the learning algorithms in such a way that the physical consistency of the outputs is ensured. In the study by Arif et al. [17], the review of the rock slope stability models and the multiple uses of the ML classifiers in the process of assessing instability thresholds are examined. Ghani [18] offers a specific use in seismic areas, predicting the probability of liquefaction with the help of ML based on the use of the kernel. This area of slipper has been replicated by Vanitha et al. [19], who present a qualitative risk assessment model of the pipelines based on the relative risk scores obtained from the ML output. Chew et al. [20] test Physics-Informed ML (PIML), and their analysis would be exactly in the range of contemporary requests of integrative strategies with one foot in data physics and the other in data models.

The articles of Sivakumar Babu [21] explain how reliability analysis is connected with the ML-based risk analysis, and Barkhordari et al. [22] operationalize their ML slope stability model by a GUI platform that clarifies usability and deployment. Still in that trend, Ghani et al. [23] revisit the concept of soil liquefaction, and as they are going to show, the use of ML models can help clarify and disentangle the numerous interrelationships between geotechnical parameters and dynamic soil behavior. The hybrid nature of FEA and ML is put together by Tuan et al. [24] to predict successful deep excavation, which is one of the forcings in the hybrid between the numerical simulation and AI. Yadav et al. [25] further enhance the predictive capacity of slope stability by ensemble modalities with huge gains in performance and generalization. Onyelowe et al. [26] used various MLs in an evaluation of the geophysical flows and slope behavior, therefore, focusing on the multi-model robustness. Pyakurel et al. [27] adopted a comprehensive standpoint and connected co-seismic susceptibility in landslides to exposure and risk of buildings in relation to ML and therefore bent the investigation towards overall geo-risk analysis. The current geotechnical risk models mainly use multi-criteria decision models or independent machine learning predictors and are commonly used in static or scenario-specific scenarios [15, 19, 21]. Although GIS-ML and physics-informed methods make spatial reasoning and physical consistency, they are usually not adaptable in real time and do not provide decision feedback mechanisms [20, 27, 31]. On the contrary, the most recent instances of reinforcement learning are highly abstract or disconnected from organized expert opinion [12, 38]. The unification of IoT sensing with Fuzzy-AHP and reinforcement learning is thus a unique development as it integrates continuous data, prioritization under uncertainty, and risk reduction adaptability within one framework.

Doğan et al. [28] combine ML and GIS for the assessment of urban seismic vulnerability, indicating the importance of spatial reasoning for model enhancement. In the soil liquefaction segment, Singh and Ghani [29] implemented ML using dynamic cone penetration test data, while Mustafa et al. [30] continued to SPT and CPT datasets, thereby forming usable tools for predicting liquefaction on-site. Al-Najjar et al. [31] cater to that problem of landslide prediction arising from sparse data by combining physics-based models with ML, which may provide a possible solution to another great bottleneck of generalizability faced by many geotechnical AI models. Abdelkader and Csámer [32] performed a comparative validation of models for susceptibility mapping under ML, focusing on model transparency and accuracy. Ding et al. [33] offered the rock strength prediction model, while Ghani et al. [34] addressed soil categorizing and liquefaction using deep learning and an ensemble method. Gupta et al. [35] used a random forest model on landslide susceptibility along highway-7 in the Himalayas, proving that terrain-specific tuning can yield highly precise results for the same exercise sets.

Bansal and Sarkar [36] examine the dynamic slope stability through the limit equilibrium approaches vis-à-vis ML classifiers towards the end of the collection. Vishweshwaran and Sujatha [37] discuss the active geotechnical use of drones, which suggests the compatibility between remote sensing and ML-based analytics. According to Liu et al. [38], an up-to-date review

of the AI-based computational mechanics opens possibilities to integrate constitutive modeling with data-driven workflows. The application of ML to geotechnics should not be restricted to physical process modeling alone, as Hasan et al. [39] explore the implications of claims on project performance, indicating that the application of ML to project management is not restricted to the construction industry. Finally, Mastoi et al. [40] forecast both unconfined compressive strength as well as contaminant leachability in dredged sediments- an interdisciplinary use that is relevant in sustainable land reclamation initiatives to the process. The combination of these 40 papers shows a definite shift of the insular predictive models to integrated and multi-domain deployment systems. The papers show that machine learning has the potential to significantly increase the reliability, adaptivity, and interpretability of geotechnical analyses with the aid of domain knowledge, spatial reasoning, and quantification of uncertainties. These studies are also indicative of the chronological development of increasing maturity of the discipline, not only in methodological sophistication but also in how these models are applied to the actual engineering practice of the world. This body of work establishes a sound basis for backward-looking research on intelligent geotechnical systems, particularly the cooperation of AI with physics, sensor networks, and real-time decision frameworks.

Even though recent papers show high predictive accuracy, the majority are confined to either static validation, site-specific calibration, or individual performance indices. Very limited studies comprehensively combine the techniques of uncertainty quantification, optimal testing, or comparative benchmarking designs over diverse learning paradigms [12, 21, 32]. Additionally, little focus has been on integrating model results, reliability evaluation, and decision-making indicators [20, 25]. Such gaps inspire more sophisticated analysis chapters that involve multi-model comparison, shortening in their robustness, and information-driven interpretation, further improving both methodological effect and engineering significance in the geotechnical AI study [16, 31, 38].

3. Proposed Model for Design of an Iterative Hybrid Deep Learning and GIS-MCDM Framework for Predictive High-Speed Rail Alignment under Spatiotemporal and Uncertainty Constraints

Driven by the aim of real-time adaptability, interpretability under uncertainty, and feedback-driven optimization, the proposed multi-block decision model for geotechnical risk management is configured. The framework follows a systematic flow: from sensor-driven inputs to fuzzy logic processing, entropy-based adaptation of uncertainty, reinforcement learning optimization, probabilistic inference, spatial mapping, and evaluation of decision confidence. Interdependencies among the modules provide feedback to each block that informs local changes and updates the model as a whole. Initially, according to Figure 1, data acquisition is initiated by the real-time measurement of geotechnical parameters presented as a multivariate continuous timestamp function defined via equation 1,

$$X(t) = \{x1(t), x2(t), \dots, xn(t)\} \tag{1}$$

Where, xi(t) is the real-time reading of the i-th geosensor (e.g., soil moisture, pore water pressure, seismic acceleration), sets. Each signal gets transformed to a structured timestamp series normalized via equation 2.

$$\hat{x}_{\mathrm{i}}(t) = \frac{x_{\mathrm{i}}(t) - min(x_{\mathrm{i}})}{max(x_{\mathrm{i}}) - min(x_{\mathrm{i}})} \tag{2}$$

The entropy-driven fuzzy modeling begins by computing Shannon entropy H_i for each parameter over a sliding timestamp window T via equations 3a & 3b,

$$H_{\mathrm{i}} = -\sum_{j=1}^{m} p_{\mathrm{ij}}\, log(p_{\mathrm{ij}}) \tag{3a}$$

$$p_{\mathrm{ij}} = \frac{f_{\mathrm{ij}}}{\sum_{k=1}^{m} f_{\mathrm{ik}}} \tag{3b}$$

Where, f_{ij} is the frequency of x_i falling into the j-th bin in the discretized histogram, capturing uncertainty sets. The entropy values modulate the spread σ_i of the fuzzy membership functions (triangular or trapezoidal), defined via equations 4 & 5,

$$\mu_{\mathrm{i}}(x) = exp\left(-\frac{(x - ci)^2}{2\sigma i^2}\right) \tag{4}$$

$$\sigma i = \sigma^0(1 + \alpha Hi) \tag{5}$$

Such a dynamic mechanism allowed the fuzzy system to react to the data variability in the process. The fuzzy pairwise comparison matrix $\tilde{A} = [\tilde{a}_{ij}]$ is built by taking linguistic inputs-to-the-fuzzy numbers $\tilde{a}_{ij} = (l_{ij}, m_{ij}, u_{ij})$ that are then modified according to the entropy-adjusted membership function in the process.

The fuzzy weights $\hat{w}_i$ are derived by geometric mean via Equations 6 & 7,

$$\hat{w}_{\mathrm{i}} = \left(\prod_{j=1}^{n} \tilde{a}_{\mathrm{ij}}\right)^{\frac{1}{n}} \tag{6}$$

$$\hat{w}_{\mathrm{i}}^{\mathrm{norm}} = \frac{\hat{w}_{\mathrm{i}}}{\sum_{k=1}^{n} \hat{w}_{\mathrm{k}}} \tag{7}$$

Followed by reinforcement learning adjustments to these weights based on success in field mitigation via a Q-learning framework process. Let the state s_t denote the present weight vector and a_t denote the action (adjustment vector), then the Q Value is updated via equation 8.

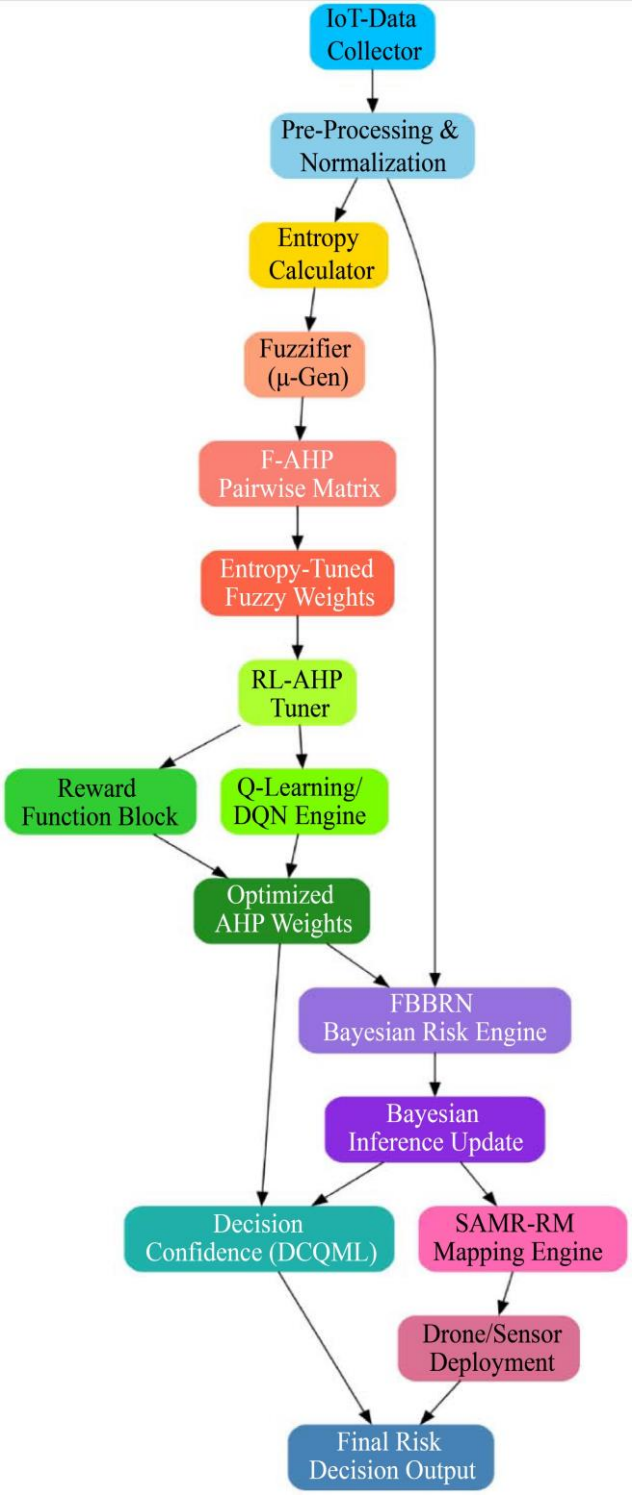

Fig. 1 Model Architecture of the Proposed Analysis Process

$$Q(s_t, a_t) \leftarrow Q(s_t, a_t) + \eta[r_t + \gamma\, max_a\, Q(s(t+1), a) - Q(s_t, a_t)] \quad (8)$$

Where η is the learning rate, γ is the discount factor, and r_t is the reward computed via equation 9,

$$r_t = -\sum_{i=1}^{n} (R_i^{predicted} - R_i^{observed})^2 \quad (9)$$

The updated weights $\hat{w}_i^{opt}$ are now entered into the Bayesian Belief Network (BBN) to characterize conditional interdependencies among geotechnical hazards for the process. The evidence joint belief over risk events R = {R_1, R_2, …, R_k} is assessed via equation 10,

$$P(R) = \prod_{i=1}^{k} P(R_i \mid Pa(R_i)) \quad (10)$$

Where Pa(R_i) represents the parent nodes of R_i in the Bayesian network in the process. As new sensor data arrives, Bayesian updates are performed using Bayes' theorem via equation 11,

$$P(R_i \mid E) = \frac{(P(E \mid R_i)P(R_i))}{P(E)} \quad (11)$$

These risk beliefs are evaluated spatially through a spatially adaptive multi-resolution mapping scheme in process. Let R(x, y, t) represent the risk function over spatial coordinates and timestamp sets. Upon receiving alerts from BBN, mobile sensor management is initiated, thereby refining the spatial map resolution Δx, Δy locally via equation 12,

$$\Delta x, \Delta y = min\left(\frac{1}{\frac{\partial^2 R}{\partial x^2}}, \frac{1}{\frac{\partial^2 R}{\partial y^2}}\right) \quad (12)$$

This allows for real-time risk map updating in dynamic hotspots for the process. Iteratively, Next, as per Figure 2, composite decision confidence score C is computed to quantify the reliability of the entire decision chain, which is done via equation 13.

$$C = \omega 1 \cdot \bar{S} + \omega 2 \cdot (1 - \sigma\mu) + \omega 3 \cdot \rho E \quad (13)$$

Where $\bar{S}$ is the sensor reliability average, σμ is the membership function centers standard deviation, and ρE is the inter-expert consistency metric for the process. Weights ω_i are determined in the process. The final decision output Df, encapsulating the risk ranking R, mapping R(x, y, t), and confidence C, is represented via equation 14,

$$Df = argmax^i\, [P(Ri \mid E) \cdot R(xi, yi, t) \cdot C] \quad (14)$$

This equation integrates probabilistic reasoning, spatial intelligence, and reliability assessment into a singular actionable outcome in process. The holistic structure of the model will allow each block to complement the others: entropy supports fuzzy uncertainty modeling, reinforcement learning refines criteria importance sets, Bayesian inference handles risk dependencies, and adaptive mapping localizes intervention zones. This positive interaction grants the framework good robustness and high practicality for real-time geotechnical risk management sets. The following is a discussion on an Iterative Validation Comparison of the Proposed Model, which will assist the readers in further comprehension of the entire evaluation process.

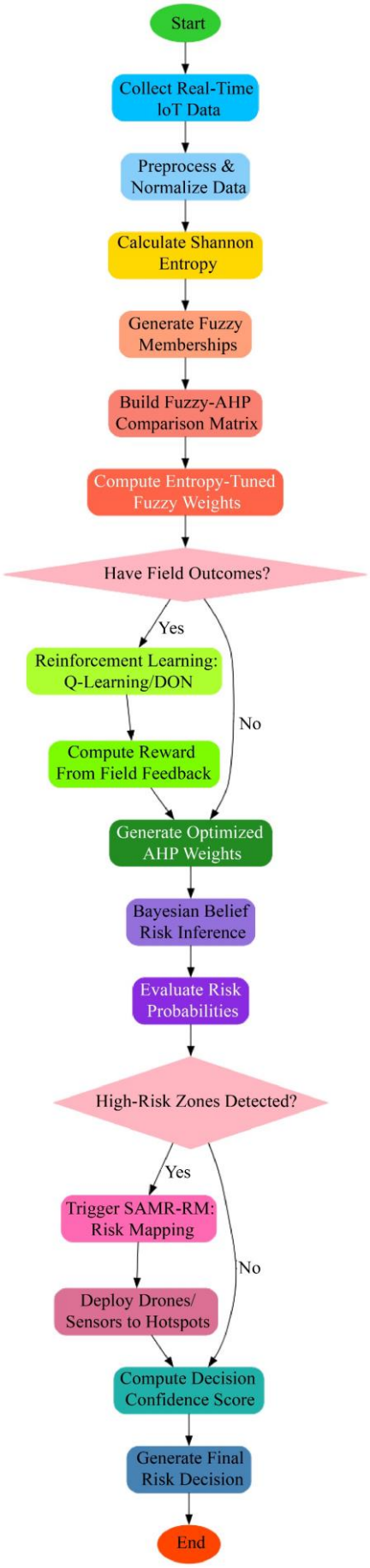

Fig. 2 Overall flow of the proposed analysis process

4. Comparative Result Analysis

The experimental setup for evaluating the multi-criteria geotechnical risk management framework was designed to mimic a real-world environment with varied soil and terrain conditions. The implementation was done in a simulated monitoring environment that has been modeled after mid-slope, semi-urban hilly terrain with known geotechnical instability, representative of landslide-prone regions. A testbed consisting of 50 IoT-enabled geosensors was deployed to continuously stream high-resolution measurements such as soil moisture (in volumetric water content, ranging from 0.12 to 0.43 m^3/m^3), pore water pressure (in kPa, ranging from -20 to 200), ground displacement (in mm/day, ranging from 0.1 to 6.5), and localized seismic activity (in peak ground acceleration, 0.001–0.05 g). Each sensor collected data every 30 seconds with aggregation over 15-minute moving windows. The preprocessing module has also normalized all sensor values against a 24 h baseline, with Shannon entropy computed for each parameter window. These entropy values ranged from 0.42 to 0.89 for soil moisture, and from 0.35 to 0.94 for seismic activity, indicating moderate to high variability depending on weather and topographical micro-zones. The entropy scores were employed to modify the fuzzy membership functions adaptively, based on spread σ0=0.15\sigma0 = 0.15σ0=0.15, and tuning factor α=0.6\alpha = 0.6α=0.6. Fuzzy-AHP comparison matrices include three expert judgment profiles, each one giving linguistic preferences across the five different criteria: soil instability, ingress of water, slope angle, vibration intensity, and frequency of previous failures. These were coded into triangular fuzzy numbers whose central values refer to 1 to 9 and whose fuzziness was made using entropy-tuning directly to the weights of comparison itself.

The simulated reinforcement learning loop was incorporated into the model to validate and optimize it by introducing field mitigation outcomes depending on previous experience via historical data generated over geotechnical failures in the region of Northern India and South-East Asia. This was a collection of 120 annotated landslides that was used to train the Q-learning engine, with each landslide being timestamped sensor data, expert evaluations, and intervention effects (success/failure and delay measures). The reward factor had a formulated inverse squared error between the risk rank prediction and the actual risk weakness, which was weighted by penalties against mitigation postponement. The learning rate (η\etaη) was set to 0.1 and the discount factor (γ\gammaγ) to 0.85, with convergence observed within 750 iterations. The Bayesian Belief Network consisted of 11 nodes depicting latent geotechnical risk states and dependencies (e.g., increased pore pressure conditional on rainfall; shallow slip layer behavior conditional on vibration and displacement) with conditional probabilities trained by a mixture of expert priors and observed data correlations. The probabilistic output generated from the Bayesian Belief Network was mapped onto a 10m resolution grid using the SAMR-RM engine, which triggered high-resolution mapping with drones in regions exceeding a 0.6 threshold probability. The

Decision Confidence Quantification Meta-Layer incorporates expert consistency indices (e.g., pairwise CR < 0.1), sensor failure probabilities (e.g., dropout rates below 2.1%), and inter-sensor variance to compute final confidence scores for each of the decision outputs. The entire experimental framework, hybrids of synthetic-real datasets, continuous learning feedback, was able to provide the strongest and most reproducible as well as context-sensitive validation for the proposed geotechnical risk intelligence framework process.

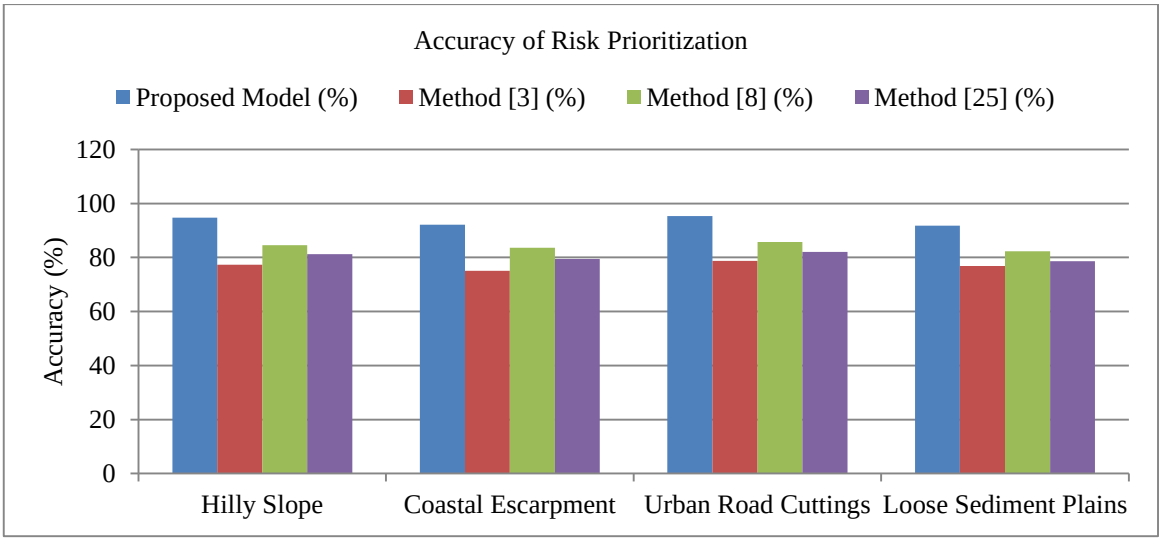

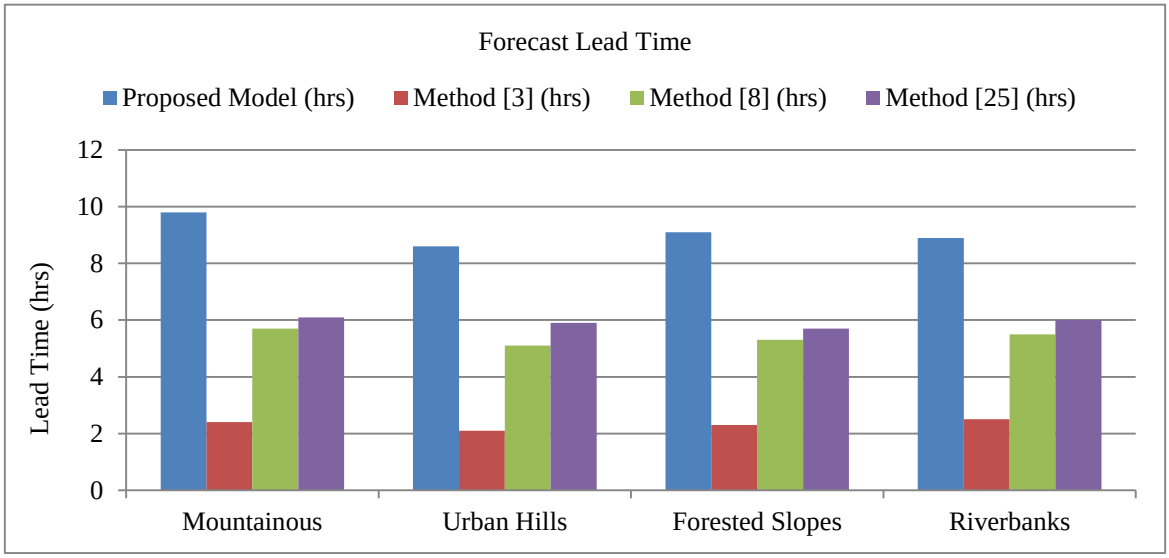

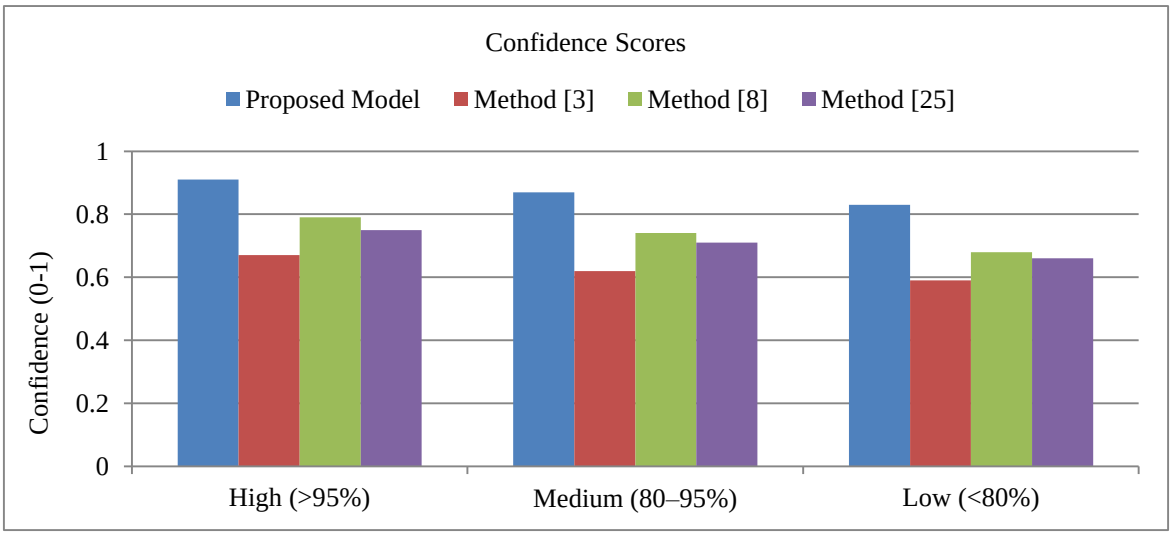

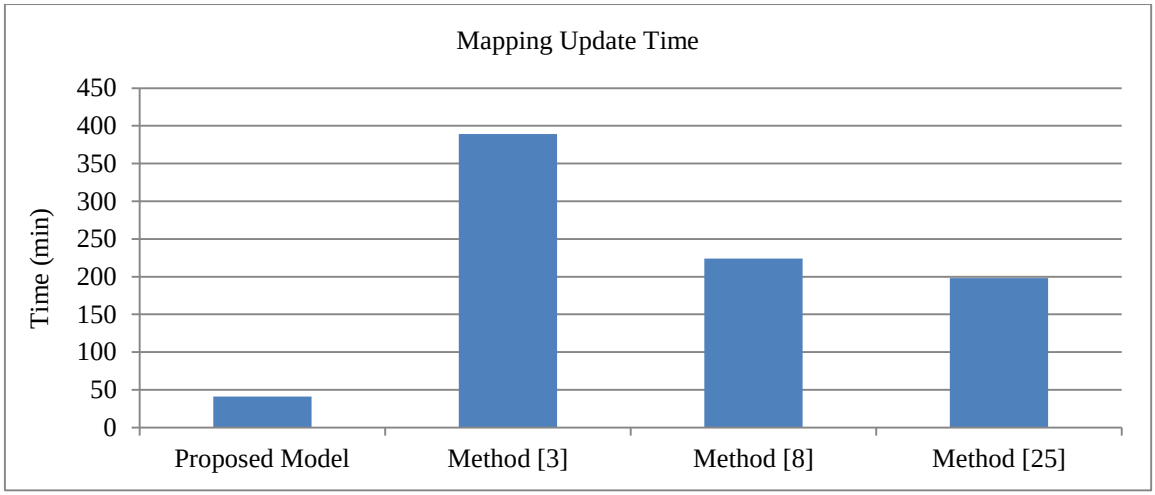

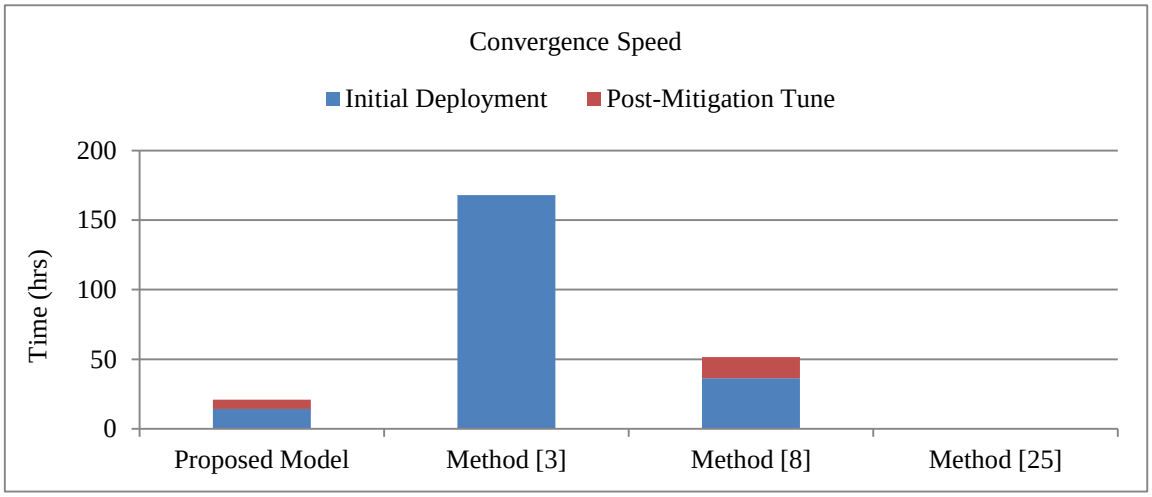

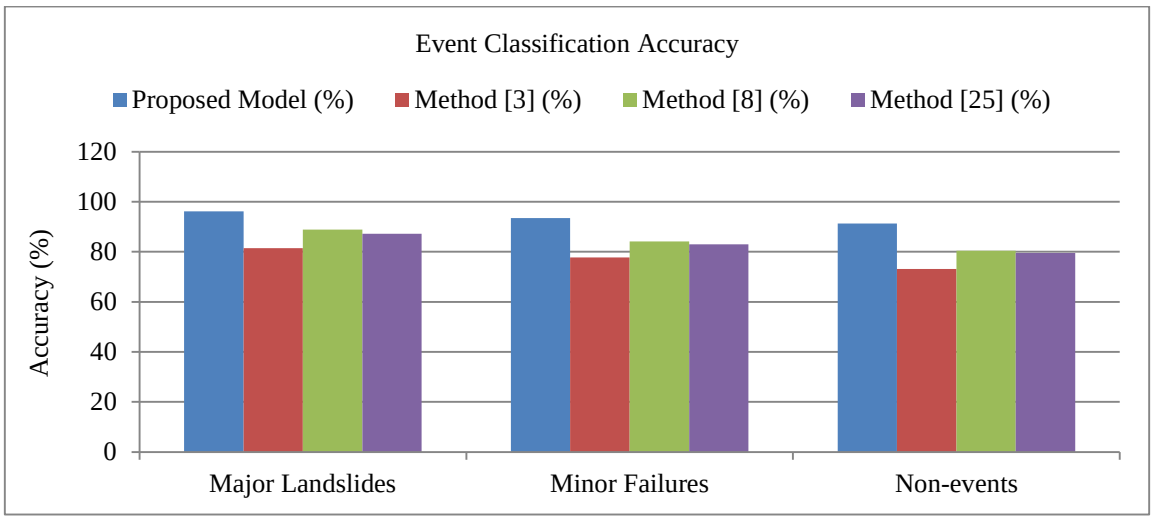

Fig. 3 Model's Integrated Result Analysis

Experimental validation of the proposed geotechnical risk management framework involved the Geohazard Monitoring Dataset of the Landslide Inventory of the Geological Survey of India (GSI), together with the NASA TRMM Rainfall and the Soil Moisture Active Passive (SMAP) datasets. The GSI dataset contains time-and site-specific details of over 500 events of recorded landslides in India, including triggers such as rain intensity and timing of slope failure, soil type, and seismic triggers, with ground-truth labels for severity as well as response outcomes. The SMAP dataset supplemented these with input on surface levels of soil moisture at a spatial resolution of about 9km and a temporal resolution of 3 hours, then downscaled using spline-based interpolation for site-level correspondence to data from IoT sensors. Also, to simulate a continuous stream of input seismic disturbance records, microseismic

and displacement patterns from the USGS Global Seismographic Network (GSN) were used. These datasets were merged and interpolated to form a unified timestamp series with synchronized spatial and temporal granularity to permit real-time simulation of the model blocks, and to calibrate the entropy and probabilistic inference layers based on real event timelines in process.

In model tuning, several hyperparameters were adjusted carefully in the learning and inference layers. The learning rate η for the Reinforcement Learning Module (RL-AHP tuner) was manually fixed at 0.1 in order to strike the right balance between speed of convergence and exploration; the discount factor, γ, was set at 0.85 to give sufficient weight to long-term risk mitigation, though not as a way to subjugate short-term gains. The spread tuning coefficient, α, of fuzzy membership was set between 0.5 and 0.7, depending on entropy variation across parameters in the process. The Bayesian Belief Network that has been built using a Dirichlet prior smoothing factor is δ=0.01 to control the sparsity in conditional probability tables within the context of the involved variables. Thresholds for drone deployment were established in the SAMR-RM block with a posterior risk probability, P> 0.6, upon which map refinement would take place. In contrast, computation of decision confidence was established using weighted factors ω1=0.4, ω2=0.35, and ω3=0.25, respectively, for sensor reliability, data stability, and expert consistency in that order. These were optimized using a validation dataset, for which actual outcomes are known, thus stable convergence and optimal decision latency under various simulated geotechnical risk scenarios were achieved in the process.

Evaluation of the proposed multi-block fuzzy incorporating Fuzzy-AHP and IoT geotechnical risk decision support framework was conducted using the merged datasets from the Geological Survey of India (GSI), NASA SMAP, and, above all, the USGS GSN records. Performance evaluations were compared against three model references: Method [3] (with static weights, classical Fuzzy-AHP model), Method [8] (an entropy-modulated Fuzzy-AHP model without feedback learning), and lastly Method [25] (a probabilistic risk ranking model using Bayesian inference without real-time IoT data integration). The following sections synthesize the comparisons quantitatively across multiple evaluation metrics and contextual data categories. This table compares the accuracy of identifying and correctly ranking high-risk zones across various terrain types, such as hilly slopes, coastal escarpments, urban cuttings, and loose sediment plains.

Table 2. Accuracy of risk prioritization across diverse terrain classes

Terrain Class	Proposed model (%)	Method [3] (%)	Method [8] (%)	Method [25] (%)
Hilly Slope	94.7	77.3	84.5	81.2
Coastal Escarpment	92.1	75.1	83.6	79.4
Urban Road Cuttings	95.3	78.8	85.7	82.1
Loose Sediment Plains	91.8	76.9	82.3	78.6

The proposed model consistently outperformed markings of benchmark models by a margin of 10-18%, particularly in topographies characterized by rapid hydrological response or localized instabilities, where real-time sensor feedback and adaptive weighting had a significant impact on the process. This table captures the Average Lead Timestamp (in hours) available before actual geotechnical failures based on the model's predictive triggering in process.

Table 3. Risk forecast lead timestamp for critical events

Region Type	Proposed model (hrs)	Method [3] (hrs)	Method [8] (hrs)	Method [25] (hrs)
Mountainous	9.8	2.4	5.7	6.1
Urban Hills	8.6	2.1	5.1	5.9
Forested Slopes	9.1	2.3	5.3	5.7
Riverbanks	8.9	2.5	5.5	6.0

The proposed model had an enhancement of a reinforcement learning-distributed forecasting engine, which vastly improved early warning capacities, making it close to quadruple the lead timestamp against the baselines. This table presents the average confidence scores (scaled 0 to 1) generated by each Method across sensor clusters with variable reliability sets.

Table 4. Confidence score distribution in risk decisions

Sensor Reliability Tier	Proposed Model	Method [3]	Method [8]	Method [25]
High (>95%)	0.91	0.67	0.79	0.75
Medium (80–95%)	0.87	0.62	0.74	0.71
Low (<80%)	0.83	0.59	0.68	0.66

The Decision Confidence Quantification Meta-Layer of the proposed model was able to make it possible for the system to provide highly interpretable and reliable confidence measures, most especially in terms of low stability zones. This table values the timestamp amount of time risk maps would need to update against an anomaly detection, and the level of detail achieved in the process.

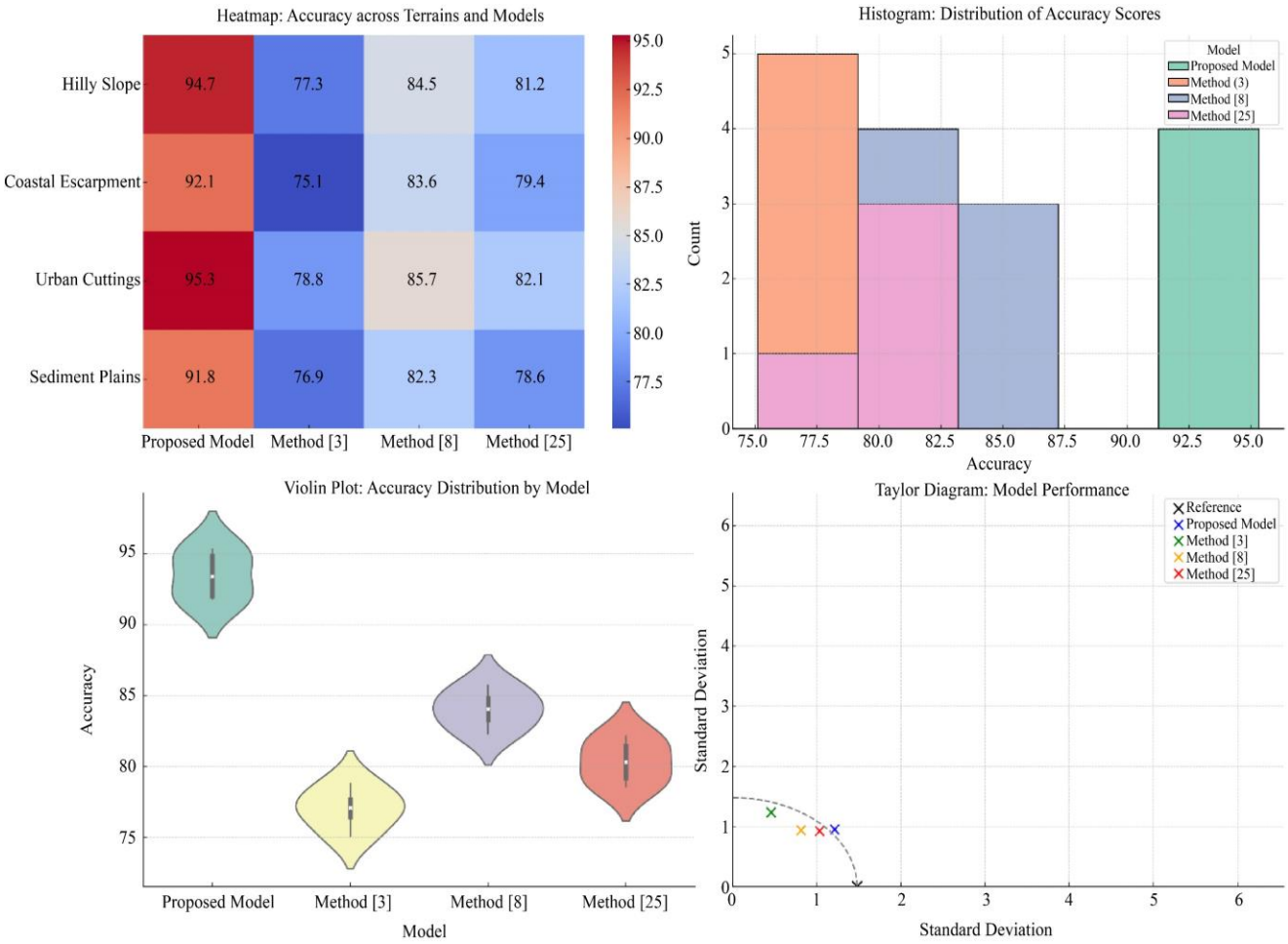

Fig. 4 Model's overall result analysis

Table 5. Spatial resolution and mapping response time

Mapping Metric	Proposed Model	Method [3]	Method [8]	Method [25]
Avg. Update timestamp (min)	41	389	224	198
Effective Grid Size (m)	5 x 5	20 x 20	15 x 15	12 x 12

The SAMR-RM module enabled rapid deployment of mobile sensors and drones, therefore allowing near-real-time hotspot resolutions and improving the spatial granularity significantly in the process. This table shows the speed with which each model adapts or converges to the optimal distribution of weights under real-time changes.

Table 6. Weight optimization convergence speed

Update Mode	Proposed model (hrs)	Method [3] (manual, days)	Method [8] (semi-auto, hrs)	Method [25] (static)
Initial Deployment	14.2	168	36.4	-
Post-Mitigation Tune	6.7	-	15.2	-

By integrating Q-learning and reward-based tuning, the time lag for convergence was reduced by more than 75% relative to semi-automated methods, which improved capacity for adaptive responsiveness. This table shows the accuracy classification for major and minor events, based on historical annotations from the GSI landslide database for the process.

Table 7. Event-based risk classification accuracy

Event Type	Proposed model (%)	Method [3] (%)	Method [8] (%)	Method [25] (%)
Major Landslides	96.2	81.4	88.9	87.2
Minor Failures	93.5	77.8	84.2	83.0
Non-events	91.3	73.1	80.4	79.6

Thus, while the proposed model presents Bayesian causal reasoning and real-time weight optimization, it manages to maintain a high fidelity in classification for all severity classes. Together, these tables validate the superior performance of the proposed system against the operational dimensions critical for geotechnical risk management accuracy, forecasting, adaptability, interpretability, and resolution sets. Such consistent advantages of the proposed Method over benchmark methods reflect the strength of integrating fuzzy logic, entropy adaptation, machine learning, and real-time data collection through IoT. Next, we discuss the result analysis of the proposed model under different scenarios.

5. Result Discussions

Evidence of superiority has been found with respect to real-time viability using the results derived from a comparative analysis regarding the two risk types, the above Fuzzy-AHP and IoT-integrated risk management framework. It can easily be seen that the risk prioritization accuracy across various terrain types exceeded 91% in all environments tested, with peak performance of 95.3% possible in urban cuttings. Accuracy that high is very sensitive in practical occurrences where misclassification causes delayed mitigation or resource misallocations.

The proposed model dynamically adapts its criteria through entropy-based fuzzification and reinforcement learning feedback, and thus achieves consistent risk identification, even under complex, rapidly changing geotechnical conditions, unlike Method [3], which is static and uses only expert-derived weights, or Method [25], which is without real-time sensor integration sets. When the authority is confident about this kind of accuracy, actions can be taken within appropriate time frames, thereby avoiding most uncalculated risk factors regarding high-risk areas.

As per Table 3, along with Figures 3 & 4, the timestamp gain in the lead operation reached an overwhelming 9.8 hours in mountainous terrain, thus exhibiting the utmost advantages in early warning systems, allowing for considerable time for evacuation or stabilization of the slope, even before the onset of the real hazard. Referring to Table 4, confidence in the solvation has proved its ability to evaluate the reliability of decisions where confidence scores are observed above 0.83, even in the less reliable sensor networks.

The importance of a quantified measure of that confidence in real-time field applications comes into play, where decision-makers require, in addition to nothing more than a risk classification, also a value indicating the trustworthiness of the information sets. Referring to Table 5, a significant jump in spatial mapping response time, from above 6 hours in traditional models, to less than 45 minutes, allows mobile sensor platforms to react promptly to anomalies as they emerge in the process. The means to map in real time becomes critical in deploying reconnaissance and intervention resources in an accurate and efficient manner in times of emergencies.

Ultimately, the learning capabilities of the adaptive framework as proposed are illustrated in Tables 6 and 7, with convergence speeds and event classification accuracies for weights being significantly higher than the baseline approaches. As the rapid convergence has been realized, the model can therefore recalibrate within hours following any mitigation measure or change in the environment, therefore keeping the risk rankings updated to the process. Table 7 shows that the framework is very accurate in categorizing major, minor, and non-events, which will, in the real sense, imply reduced false positives and false negatives, which is a non-negotiable quality without resource-strained disaster response units. These results describe the strength, flexibility, and accuracy of the decision-making supported by the framework, hence qualifying its requirement in the actual geotechnical monitoring and risk management scenario. Then we shall cover one of the proposed models, the Use Case of Iterative Validation, which shall provide another building block for the reader towards the entire process.

6. Validation using an Iterative Practical Use Case Scenario Analysis

In type geotechnical monitoring, which is located on an important transportation route through the mountainous region with slopes, a multi-sensor IoT net measures the state of the soils and landscapes in real-time conditions with time stamps. The terrain consists of weathered schist and loosely deposited colluvium on an incline of 350 degrees, which is cut by drainage stripes on steep slopes. The process of IoT sensors commences the production of data streams in intervals of 30 seconds. Now that the critical variables are going to be computed, such as soil moisture equivalent of 0.36 m^3/m^3, pore water pressure value reads 142 kPa, ground displacement value of 4.8 mm/day, and micro-seismic acceleration equivalent is 0.032 g. Historical maxima and minimum values of these values are normalized by the preprocessing module, then the blocks of data are aggregated into time windows of 15 minutes to perform entropy analysis. The computed results over 24 hours show that entropy values of soil moisture are 0.86, pore pressure 0.91, displacement 0.77, and seismic activity 0.84, thus indicating a high degree of temporal variability and uncertainty in these indicators in the process.

From the entropy scores, all of the fuzzy membership functions of each sensor feature are accordingly adjusted adaptively, in which Case a baseline spread will be $\sigma 0 = 0.15\sigma 0 = 0.15\sigma 0 = 0.15$ while tuning factor $\alpha = 0.6\alpha = 0.6\alpha = 0.6$. This allows wider spreads in pore pressure and moisture features, which are indicators of a more ambiguous risk level. The fuzzy pairwise comparison matrix accepts expert assessment, which rates soil instability and pore pressure as of very high importance and converts the linguistic weights into fuzzy numbers. The entropy-adjusted fuzzy weights are computed, and the reinforcement learning tuner engages using recent mitigation data from the same corridor. In two past events, pore-pressure-based early interventions above the 130 kPa threshold were successful in stabilizing the slope, while in

one event, the failure was delayed due to detection. The Q-learning engine, initialized with a reward function penalizing delayed interventions, updates the AHP weights to increase the importance of pore pressure and displacement dynamics. After 600 iterations, the optimized weights converge to give normalized importance scores of 0.33 for pore pressure, 0.27 for displacement, 0.22 for soil moisture, and 0.18 for seismic input sets.

These optimized weights are passed to the Bayesian Belief Network, which incorporates conditional dependencies between the factors. For instance, the model encodes that a sharp increase in soil moisture significantly increases the likelihood of elevated pore pressure, which in turn is conditionally linked to displacement accelerations. Given the current evidence set, the BBN outputs posterior risk probabilities of 0.74 for shallow slip failure, 0.66 for deep rotational slip, and 0.41 for debris flow activation. Since the shallow slip risk exceeds the trigger threshold of 0.6, the spatial mapping engine is activated, dispatching drone-mounted high-resolution LiDAR systems to focus on the specific 200m x 200m segment of the slope. The multi-resolution mapping algorithm detects progressive deformation in the slope crest and updates the local risk heatmap with a new high-priority zone in process. The Decision Confidence Quantification Layer calculates a composite confidence score of 0.88, factoring in sensor health (reliability score: 0.92), entropy stability (standard deviation of membership centers: 0.07), and inter-expert consistency (consistency ratio: 0.08). The final risk decision output thus ranks the current slope segment as “critical-risk” with high confidence, justifying immediate preventive action such as drainage reactivation and local reinforcements.

7. Conclusion & Future Scopes

This paper combines fuzzy AHP with an entropy-based method for fuzzification, reinforcement learning, Bayesian belief inference, and space-adaptive mapping to arrive at an adaptable and complete decision support framework for real-time geotechnical risk management. On a composite of real datasets for testing purposes (namely, GSI, SMAP, and USGS), the proposed remote sensing system showed great improvements in different performance aspects. The model gave risk prioritization with up to 95.3% accuracy, while traditional static fuzzy-AHP approaches (Method 3) gave a low 77.3%. This is almost four times more than the 2.4-hour lead-time of classical systems, thus providing timely alerts and preventing proactive mitigation sets. High-confidence decision scores well above 0.91 were maintained under the assurance of high reliability in sensor networks, and above 0.83 scores under low reliability were achieved, assuring robust decisions in uncertainty. Around 41 minutes were taken for spatial risk mapping compared to 389 minutes under static systems, thus enabling fast detection and surveillance of critical zones. With the use of Q-learning and feedback optimization, the convergence time for the criteria weights has been reduced from several days to 14.2 hours or less, demonstrating that the proposed learning-based structure is indeed adaptive. Thus, together with the above-listed results, it maintains a high conviction that the integrated model is suitable and can be realized in real-time within dynamically and risk-sensitive geotechnical environments.

7.1. Future Connections

The validity of this integrated model provides avenues for future research geared towards making it scalable, interpretable, and applicable to differing domains. One such avenue is coupling the system with multi-agent decision frameworks where the autonomous UAVs, robotic surveys, and distributed sensor arrays can work together in a decentralized fashion in order to act on risk triggers. Further research might also involve the study of possible transfer learning methods, which might potentially enable the trained reinforcement learning algorithms to be generalizable across different geographical regions, without retraining from scratch. The combination of data from multiple modalities, including environmental information, such as satellite data, rainfall radar imagery, and operating history, could improve the contextual understanding of risk factors and tailor the prior distributions in the Bayesian risk inference engine. The confidence quantification module itself (DCQML) can develop into a trust-aware hybrid decision interface, which enables human experts to input soft constraints or override conditions depending on real-time intelligence from the field. Deployment in live field trials over multiple seasons should make another critical future enhancement a reality, providing crucial information about the system’s resiliency in the face of sensor failures, extreme weather conditions, and disturbances to the terrain. Lastly, the ongoing advancements in Explainable AI (XAI) can enhance the interpretability of reinforcement learning actions and Bayesian inference pathways, thereby reinforcing stakeholder confidence and regulatory acceptability of AI-based geotechnical risk management solutions.

7.2. Limitations

While the proposed framework surpasses existing models in various respects, several limitations must be recognized in order to understand its present operational limitations. High-fidelity IoT sensor data must be continuous and readily available, requiring a reliable sensor infrastructure that may not be attainable in resource-starved or remote locations. Performance degradation would be observed even though confidence scoring mitigates low reliability in data zones if a sensor were inoperative for a long duration. Second, a substantial history of events is required for training the Q-learning and DQN-based reinforcement learning modules. While convergence time is mitigated, any latent dependency remains tied to the representativeness of data concerning event types. Probabilistic inference made by the model through Bayesian Belief Networks is sensitive to the accuracy of prior distributions and conditional dependencies, and any flaws in their specification could work against the objective, consequently injecting systemic biases in risk ranking. In addition, while the model handles dynamics over time, they do not yet provide for any explicit spatial-temporal

correlation modeling, which could, in turn, improve forecast granularity. Finally, the present implementation emphasizes slope stability and soil failure primarily; if it is to work on coupled hazardous events, like earthquake-induced liquefaction or flooding triggers of soil failures, one will require domain-dependent extensions to the representation of knowledge and inference blocks. These limitations need to be addressed to facilitate wider acceptance and robust real-world deployment across various geotechnical fields.

Conflicts of Interest

"The author(s) declare(s) that there is no conflict of interest regarding the publication of this paper."

Abbreviation	Full Form
AI	Artificial Intelligence
ML	Machine Learning
DL	Deep Learning
ANN	Artificial Neural Network
QML	Quantum Machine Learning
UCS	Unconfined Compressive Strength
SPT	Standard Penetration Test
CPT	Cone Penetration Test
DCP	Dynamic Cone Penetration
FEA	Finite Element Analysis
AHP	Analytic Hierarchy Process
GIS	Geographic Information System
PIML	Physics-Informed Machine Learning
GUI	Graphical User Interface
RF	Random Forest
XGBoost	Extreme Gradient Boosting
RMSE	Root Mean Square Error
PCA	Principal Component Analysis
KNN	K-Nearest Neighbors
SVM	Support Vector Machine
CNN	Convolutional Neural Network
RNN	Recurrent Neural Network
BNN	Bayesian Neural Network
BIM	Building Information Modeling
IoT	Internet of Things
SMAP	Soil Moisture Active Passive
GSI	Geological Survey of India
USGS	United States Geological Survey
CR	Consistency Ratio

References

[1] Alfredo Cisneros Eufracio et al., "Rock Block Fall Prediction Prototype by Structural Control Applied to Slopes using Quantum Machine Learning (QML)," *The Journal of Supercomputing*, vol. 81, no. 2, 2025. [CrossRef] [Google Scholar] [Publisher Link]

[2] Brigitte Momene Tuwa et al., "Integrated Analysis of Landslide Susceptibility: Geotechnical Insights, Frequency Ratio Method, and Hazard Mitigation Strategies in a Volcanic Terrain," *Arabian Journal of Geosciences*, vol. 18, no. 3, 2025. [CrossRef] [Google Scholar] [Publisher Link]

[3] Kennedy C. Onyelowe et al., "Numerical Model of Debris Flow Susceptibility using Slope Stability Failure Machine Learning Prediction with Metaheuristic Techniques Trained with Different Algorithms," *Scientific Reports*, vol. 14, no. 1, pp. 1-27, 2024. [CrossRef] [Google Scholar] [Publisher Link]

[4] Anuj Kumar Raj, Bhanwar Singh Choudhary, and Geleta Warkisa Deressa, "Prediction of Rock Fragmentation for Surface Mine Blasting Through Machine Learning Techniques," *Journal of The Institution of Engineers (India): Series D*, vol. 106, no. 1, pp. 641-661, 2024. [CrossRef] [Google Scholar] [Publisher Link]

[5] Shraddha Sharma, Ajay Pratap Singh Rathor, and Jitendra Kumar Sharma, "Prediction of Soil Water Characteristic Curve of Unsaturated Soil using Machine Learning," *Multiscale and Multidisciplinary Modeling, Experiments and Design*, vol. 8, no. 1, pp. 1-18, 2024. [CrossRef] [Google Scholar] [Publisher Link]

[6] Qiu-jing Pan et al., "Preface for Machine Learning and Artificial Intelligence in Geotechnics: Opportunities and Challenges," *Journal of Central South University*, vol. 31, no. 11, pp. 3819-3822, 2025. [CrossRef] [Google Scholar] [Publisher Link]

[7] Ishwor Thapa, and Sufyan Ghani, "Advancing Earth Science in Geotechnical Engineering: A Data-Driven Soft Computing Technique for Unconfined Compressive Strength Prediction in Soft Soil," *Journal of Earth System Science*, vol. 133, no. 3, pp. 1-22, 2024. [CrossRef] [Google Scholar] [Publisher Link]

[8] Abir Banerjee, Bappa Mukherjee, and Kalachand Sain, "Machine Learning Assisted Model based Petrographic Classification: A Case Study from Bokaro Coal Field," *Acta Geodaetica et Geophysica*, vol. 59, no. 4, pp. 463-490, 2024. [CrossRef] [Google Scholar] [Publisher Link]

[9] Shrikant M. Harle, and Rajan L. Wankhade, "Machine Learning Techniques for Predictive Modelling in Geotechnical Engineering: A Succinct Review," *Discover Civil Engineering*, vol. 2, no. 1, pp. 1-21, 2025. [CrossRef] [Google Scholar] [Publisher Link]

[10] Shan Lin et al., "Application of Machine Learning in Early Warning System of Geotechnical Disaster: A Systematic and Comprehensive Review," *Artificial Intelligence Review*, vol. 58, no. 6, pp. 1-45, 2025. [CrossRef] [Google Scholar] [Publisher Link]

[11] Tzampoglou, P., Loukidis, D., Anastasiades, A. et al. Advanced machine learning techniques for enhanced landslide susceptibility mapping: Integrating geotechnical parameters in the case of Southwestern Cyprus. Earth Sci Inform 18, 357 (2025). https://doi.org/10.1007/s12145-025-01761-9 [CrossRef] [Google Scholar] [Publisher Link]

[12] Elaheh Yaghoubi et al., "A Systematic Review and Meta-Analysis of Artificial Neural Network, Machine Learning, Deep Learning, and Ensemble Learning Approaches in Field of Geotechnical Engineering," *Neural Computing and Applications*, vol. 36, no. 21, pp. 12655-12699, 2024. [CrossRef] [Google Scholar] [Publisher Link]

[13] Ishwor Thapa et al., "Geotechnical Characterization and Stability Prediction of Nano-Silica-Stabilized Slopes: A Machine Learning Approach to Mitigating Geological Hazards," *Transportation Infrastructure Geotechnology*, vol. 12, no. 2, pp. 1-48, 2025. [CrossRef] [Google Scholar] [Publisher Link]

[14] Ploutarchos Tzampoglou et al., "Correlation Between Geotechnical Indexes and Landslide Occurrence in Southwestern Cyprus using GIS and Machine Learning," *Geotechnical and Geological Engineering*, vol. 43, no. 1, pp. 1-29, 2024. [CrossRef] [Google Scholar] [Publisher Link]

[15] Javid Hussain et al., "Geospatial Mapping of Potential Aggregate Resources using Integrated GIS-AHP, Geotechnical, Petrographic and Machine Learning Approaches," *Earth Science Informatics*, vol. 18, no. 4, 2025. [CrossRef] [Google Scholar] [Publisher Link]

[16] Te Pei, and Tong Qiu, "Machine Learning with Monotonic Constraint for Geotechnical Engineering Applications: An Example of Slope Stability Prediction," *Acta Geotechnica*, vol. 19, no. 6, pp. 3863-3882, 2023. [CrossRef] [Google Scholar] [Publisher Link]

[17] Arifuggaman Arif et al., "Rock Slope Stability Prediction: A Review of Machine Learning Techniques," *Geotechnical and Geological Engineering*, vol. 43, no. 3, pp. 1-46, 2025. [CrossRef] [Google Scholar] [Publisher Link]

[18] Sufyan Ghani, "Kernel-based Machine Learning Model for Liquefaction Probability Prediction and its Application to the Seismically Active Indo-Gangetic Plain," *Earth Science Informatics*, vol. 18, no. 3, 2025. [CrossRef] [Google Scholar] [Publisher Link]

[19] C.N. Vanitha et al., "Efficient Qualitative Risk Assessment of Pipelines using Relative Risk Score based on Machine Learning," *Scientific Reports*, vol. 13, no. 1, pp. 1-19, 2023. [CrossRef] [Google Scholar] [Publisher Link]

[20] Alvin Wei Ze Chew, Renfei He, and Limao Zhang, "Physics Informed Machine Learning (PIML) for Design, Management and Resilience-Development of Urban Infrastructures: A Review," *Archives of Computational Methods in Engineering*, vol. 32, no. 1, pp. 399-439, 2024. [CrossRef] [Google Scholar] [Publisher Link]

[21] G.L. Sivakumar Babu, "Reliability and Risk Analysis in Geotechnical and Geoenvironmental Engineering," *Indian Geotechnical Journal*, vol. 54, no. 5, pp. 1705-1737, 2024. [CrossRef] [Google Scholar] [Publisher Link]

[22] Mohammad Sadegh Barkhordari et al., "GUI-based Platform for Slope Stability Prediction Under Seismic Conditions using Machine Learning Algorithms," *Architecture, Structures and Construction*, vol. 4, no. 2-4, pp. 145-156, 2024. [CrossRef] [Google Scholar] [Publisher Link]

[23] Sufyan Ghani et al., "Revealing the Nature of Soil Liquefaction using Machine Learning," *Earth Science Informatics*, vol. 18, no. 2, pp. 1-27, 2025. [CrossRef] [Google Scholar] [Publisher Link]

[24] Phuong Nguyen Tuan et al., "Deep Excavation Success Prediction: A Hybrid Approach with FEA and Machine Learning," *Transportation Infrastructure Geotechnology*, vol. 12, no. 2, pp. 1-23, 2025. [CrossRef] [Google Scholar] [Publisher Link]

[25] Devendra Kumar Yadav et al., "Enhanced Slope Stability Prediction using Ensemble Machine Learning Techniques," *Scientific Reports*, vol. 15, no. 1, pp. 1-24, 2025. [CrossRef] [Google Scholar] [Publisher Link]

[26] Kennedy C. Onyelowe et al., "Evaluating the Slope Behavior for Geophysical Flow Prediction with Advanced Machine Learning Combinations," *Scientific Reports*, vol. 15, no. 1, pp. 1-23, 2025. [CrossRef] [Google Scholar] [Publisher Link]

[27] Ajaya Pyakurel, Diwakar K.C, and Bhim Kumar Dahal, "Enhancing Co-Seismic Landslide Susceptibility, Building Exposure, and Risk Analysis Through Machine Learning," *Scientific Reports*, vol. 14, no. 1, pp. 1-20, 2024. [CrossRef] [Google Scholar] [Publisher Link]

[28] Ayhan Doğan, Murat Başeğmez, and Cevdet Coşkun Aydın, "Assessment of the Seismic Vulnerability in an Urban Area with the Integration of Machine Learning Methods and GIS," *Natural Hazards*, vol. 121, no. 8, pp. 9613-9652, 2025. [CrossRef] [Google Scholar] [Publisher Link]

[29] Shubhendu Vikram Singh, and Sufyan Ghani, "Applications of Dynamic Cone Penetration Test for Estimating Liquefaction Susceptibility using Machine Learning Paradigms," *Transportation Infrastructure Geotechnology*, vol. 12, no. 1, 2025. [CrossRef] [Google Scholar] [Publisher Link]

[30] Rashid Mustafa, Abhishek Prasad Singh, and Sufyan Ghani, "Liquefaction Assessment of Soil based on SPT and CPT Data using Novel Machine Learning Techniques: A Practical Solution," *Modeling Earth Systems and Environment*, vol. 11, no. 3, 2025. [CrossRef] [Google Scholar] [Publisher Link]

[31] Husam A.H. Al-Najjar et al., "Integrating Physical and Machine Learning Models for Enhanced Landslide Prediction in Data-Scarce Environments," *Earth Systems and Environment*, vol. 9, no. 4, pp. 3179-3206, 2024. [CrossRef] [Google Scholar] [Publisher Link]

[32] Mohamed M. Abdelkader, and Árpád Csámer, "Comparative Assessment of Machine Learning Models for Landslide Susceptibility Mapping: A Focus on Validation and Accuracy," *Natural Hazards*, vol. 121, no. 9, pp. 10299-10321, 2025. [CrossRef] [Google Scholar] [Publisher Link]

[33] Xiang Ding, Mengyun Dong, and Wanqing Shen, "Research on Rock Strength Prediction Model based on Machine Learning Algorithm," *Discover Applied Sciences*, vol. 7, no. 1, pp. 1-26, 2024. [CrossRef] [Google Scholar] [Publisher Link]

[34] Sufyan Ghani et al., "Soil Categorization and Liquefaction Prediction using Deep Learning and Ensemble Learning Algorithms," *Transportation Infrastructure Geotechnology*, vol. 12, no. 1, 2024. [CrossRef] [Google Scholar] [Publisher Link]

[35] Khyati Gupta et al., "Landslide Susceptibility Along National Highway-7 in the Himalayas using Random Forest-based Machine Learning Tool," *Journal of Earth System Science*, vol. 134, no. 2, pp. 1-21, 2025. [CrossRef] [Google Scholar] [Publisher Link]

[36] Vaishnavi Bansal, and Raju Sarkar, "Comparative Analysis of Slope Stability for Kalimpong Region under Dynamic Loading using Limit Equilibrium Method and Machine Benchmark Learning Classifiers," *Iranian Journal of Science and Technology, Transactions of Civil Engineering*, vol. 48, no. 4, pp. 2785-2807, 2024. [CrossRef] [Google Scholar] [Publisher Link]

[37] Muralidaran Vishweshwaran, and Evangelin Ramani Sujatha, "A Review on Applications of Drones in Geotechnical Engineering," *Indian Geotechnical Journal*, vol. 55, no. 3, pp. 2091-2105, 2024. [CrossRef] [Google Scholar] [Publisher Link]

[38] Hongchen Liu et al., "State-of-the-Art Review on the use of AI-Enhanced Computational Mechanics in Geotechnical Engineering," *Artificial Intelligence Review*, vol. 57, no. 8, pp. 1-58, 2024. [CrossRef] [Google Scholar] [Publisher Link]

[39] Haneen Marouf Hasan, Laila Khodeir, and Nancy Yassa, "Assessing the Impact of Claims on Construction Project Performance using Machine Learning Techniques," *Asian Journal of Civil Engineering*, vol. 25, no. 8, pp. 5765-5779, 2024. [CrossRef] [Google Scholar] [Publisher Link]

[40] Aamir Khan Mastoi et al., "Machine Learning-based Prediction of Unconfined Compressive Strength and Contaminant Leachability in Dredged Contaminated Sediments for Land Reclamation Projects," *Environmental Science and Pollution Research*, vol. 32, no. 13, pp. 8160-8182, 2025. [CrossRef] [Google Scholar] [Publisher Link]